PRAMANA
— journal of
physics

© Printed in India

Vol. 44, No. 6,
June 1995
pp. 535–544

Measurement and analysis of alpha particle induced reactions on gold

D J SHAH, H B PATEL, N L SINGH, S MUKHERJEE* and
S N CHINTALAPUDI**
Physics Department, M. S. University, Baroda 390002, India
*School of studies in Physics, Vikram University, Ujjain 456010, India
**IUC-DAEF Calcutta Centre, 3/LB-8 Bidhan Nagar, Calcutta 700091, India

MS received 30 August 1994; revised 20 February 1995

Abstract. Stacked foil activation technique and Ge(Li) gamma ray spectroscopy have been used for the measurement of excitation functions of $^{197}Au(\alpha, xn)$ $(x = 1-3)$, $^{197}Au(\alpha, 2pn)$ and $^{197}Au(\alpha, \alpha n)$ reactions up to 50 MeV. The experimental cross-sections were compared with the predictions of pre-equilibrium hybrid model, as well as with the more recent index model. A general agreement was found in all reactions using initial exciton number $n_0 = 4(4p0h)$ except for $^{197}Au(\alpha, n)$ reaction, where index model gives fairly good agreement with $n_0 = 5(5p0h)$.

Keywords. Nuclear reactions; $^{197}Au(\alpha, xnypz\alpha)$; stacked foil activation technique; $E_\alpha \leqslant 50$ MeV; hybrid and index models.

PACS No. 25·60

1. Introduction

Statistical model code which combine precompound and compound decay channels has proven to be successful in a wide range of projectile energies. Most of these models are semiclassical and have been used with considerable success in describing experimental data pertaining to the equilibration process, mainly the forward peaked hard component observed in the continuous spectra of light ejectiles and the high energy tail seen in the excitation functions. Apart from these semi-classical models [1–10], work is in progress to give a full quantum mechanical picture in the framework of multistep direct and multistep compound nucleus theories proposed by Feshbach *et al* [11] and others [12–15]. Quantum mechanical theories are not applied to routinely measurable pre-equilibrium cross-sections but they support the foundations on which the classical models are built. As a result, a number of formulations, the hybrid model of Blann [4], the exciton model of Gadioli *et al* [5], index model of Ernst *et al* [10] and many other models [16, 17] have emerged as descendents to Griffin's statistical model of intermediate structure. All these models have the common feature that they group the many body states of equilibrating system according to the exciton numbers and particle-hole densities to estimate the occurrence of configuration capable of pre-compound particle emission. There are some conceptual differences between the hybrid and exciton models. The long-standing controversy on the basic viewpoints was resolved by Bisplinghoff [18] on the basis of configuration mixing and reported different physics and approximations. In the hybrid model no intrinsic configuration mixing is assumed while full configuration mixing is inherent in the exciton model. On the other hand Ernst *et al* [10] proposed a model of independently interacting excitons,

known as index model in which it is shown that each generation in the framework of exciton model predicts the exclusive emission spectra which can easily be converted into residual nucleus population probabilities. It is shown that three stages are sufficient to describe the single and multinucleon emissions to all the orders of practical importance.

Two of the many models discussed above received greater attention because of their simplicity and transparency and have been improved over the years by their proponents. These are hybrid [4] and index models [10]. In both these model codes, at the end of the precompound stages, the equilibrated compound nucleus is calculated using the Weisskopf–Ewing formalism [19] and added incoherently to the pre-equilibrium contributions, so that the theoretical excitation function can be directly compared with the experimental ones.

Indeed large experimental data are available in literature [20–23] for alpha induced reactions on gold mostly using Ge(Li) detectors but there are large discrepancies in the cross-section values for the same reaction. In this context the present investigation was undertaken with two aims. (1) To improve the quality of existing data. (2) To compare the experimental results so obtained with the theoretical predictions based on the up-dated hybrid as well as index models.

2. Experimental procedures

Excitation functions for the reaction residues ^{200}Tl, ^{199}Tl, ^{198}Tl, ^{198}Au and ^{196}Au in the alpha particle induced reaction on ^{197}Au, were measured using stacked foil activation technique and Ge(Li) gamma ray spectroscopy (2·0 keV FWHM for 1332 keV photons of ^{60}Co). Spectroscopically-pure gold foils of purity greater than 99·99% and thickness 24 mg/cm^2 have been used as target in the stacks together with aluminium degraders of varying thicknesses to reduce the beam energy to desired levels. Two independent irradiations were carried out at the VECC Calcutta, India using 40 MeV and 50 MeV alpha particles respectively. Copper foils of thicknesses 23 mg/cm^2 and 8·9 mg/cm^2 were used as flux monitor [24]. The average beam energy incident upon a given foil, degrader and monitor was calculated from the stopping power tables of Williamson *et al* [25]. The beam is totally stopped in the electrically insulated foil stack which is itself serving as a Faraday-cup. The beam currents on the targets were kept of the order of 250 nA. The residual nuclei were identified using their characteristic gamma rays as

Table 1. Nuclear data used for the identification of residual nuclei [26].

Reaction	Q-value (MeV)	Half life $T_{1/2}$	Gamma ray energy E_γ(keV)	% Abundance (θ_γ)
^{197}Au(α, n)^{200}Tl	−9·73	26·1 h	368	88·0 ± 0·9
^{197}Au(α, $2n$)^{199}Tl	−17·80	7·42 h	455	12·0 ± 0·6
^{197}Au(α, $3n$)^{198}Tl	−25·87	5·3 h	676	10·4 ± 0·7
^{197}Au(α, $2pn$)^{198}Au	−23·78	2·69 d	412	95·5 ± 1·8
^{197}Au(α, αn)^{196}Au	−8·00	6·15 d	356	87·0 ± 1·1
Monitor reaction				
^{65}Cu(α, $2n$)^{67}Ga	−14·1	78·26 h	300	19·03 ± 1·39

mentioned in table 1 [26]. The energy and efficiency calibration of the detector were performed with a calibrated ^{152}Eu multigamma source obtained from the Radio-Chemistry Division at VECC, Calcutta. The formula used for the determination of cross-section is given in our earlier papers [27, 28]

$$\sigma = \frac{A_\gamma A_{gm} \lambda}{\Phi \theta_\gamma p_\gamma w_i p_i N_{av.} (1 - e^{-\lambda t_i}) e^{-\lambda t_w} (1 - e^{-\lambda t_c})}$$

where, σ is the cross-secion, A_γ is the photo peak area of the characteristic gamma ray of the residual nucleus, A_{gm} is the gram atomic weight of the target element, λ is the disintegration constant of the residual nucleus, Φ is the flux of the incident particle, w_i is the weight per unit area of the target foil in g/cm^2, p_i is the fractional abundance by weight of the target isotope of interest, θ_γ is the fractional abundance of characteristic gamma rays emitted per decay of the residual nucleus, p_γ is the photopeak efficiency of the gamma ray, t_i, t_w and t_c are the periods of irradiation, waiting and counting respectively.

3. Results and discussion

The measured cross-section of the reactions ^{197}Au$(\alpha, xn)^{201-x}$Tl$(x = 1-3)$, ^{197}Au$(\alpha, 2pn)^{198}$Au and ^{197}Au$(\alpha, \alpha n)^{196}$Au have been listed in table 2. The total error in the experimental cross-section is contributed by photo peak area (1–4%), detector efficiency (3–4%), uniformity of the foil thickness (1–2%), spectroscopic data (1–7%) and standard deviation (10%) of the monitor cross-section from which the flux is deduced. The relative errors which affect the shape of the excitation function is about 6%, the absolute errors on the magnitude of the cross-section is thus less than 13% in the present measurement.

Five reactions studied in gold are compared with previous measurements [20–23] as shown in figures 1–5. Lanzafame and Blann [20] used both NaI crystal and Ge(Li)

Table 2. Cross-section of the alpha-induced reaction on ^{197}Au.

E_α(MeV)	σ(mb)	σ(mb)	σ(mb)	σ(mb)	σ(mb)
Target nucleus	^{197}Au	^{197}Au	^{197}Au	^{197}Au	^{197}Au
Reaction	(α, n)	$(\alpha, 2n)$	$(\alpha, 3n)$	$(\alpha, 2pn)$	$(\alpha, \alpha n)$
Product nucleus	^{200}Tl	^{199}Tl	^{198}Tl	^{198}Au	^{196}Au
19·5	13·2 ± 1·5	44·8 ± 5·41			
20·9	19·5 ± 2·22	110·0 ± 13·28			
24·7	15·8 ± 1·8	332·0 ± 40·10			
27·0	12·3 ± 1·4	580·0 ± 70·06			
31·9	6·8 ± 0·77	310·0 ± 37·74	380·0 ± 47·42		4·18 ± 0·46
32·2	6·1 ± 0·69	297·0 ± 35·87	470·0 ± 58·65		5·33 ± 0·59
37·8	4·4 ± 0·5	125·0 ± 15·10	1110·0 ± 138·52	1·25 ± 0·15	16·20 ± 1·81
38·0	4·2 ± 0·47	110·0 ± 13·28	1050·0 ± 131·04	1·30 ± 0·15	17·40 ± 1·94
42·8	3·3 ± 0·37	82·4 ± 9·95	760·0 ± 94·84	2·10 ± 0·25	34·20 ± 3·83
47·2	2·9 ± 0·33	53·7 ± 6·48	315·0 ± 39·31	3·40 ± 0·40	43·50 ± 4·87

detector for measurement of gamma activities and the reported uncertainty in their measurement was quoted as 20%. Kurz *et al* [21] studied reactions up to 43 MeV, employing a small volume (7 cc) Ge(Li) detector with a resolution of 4·2 keV for the 1332 keV photons of ^{60}Co. The experimental errors in the cross-section were mentioned as less than 10%, but it is not mentioned whether or not this includes the uncertainty in the monitor cross-section used for flux measurement as well as the errors in spectroscopic data. Whereas excluding the above mentioned errors the uncertainty in the present measurement becomes about 6%. Capurro *et al* [22] measured the reactions up to 55 MeV using an intrinsic Ge-detector. The overall error in their measurement varied in the range 24 to 37%. Bhardwaj *et al* [23] measured the reactions up to 40 MeV using HPGe detector. The reported values of Capurro *et al* and Bhardwaj *et al* differ by more than 50% around 30 MeV and the deviation is larger at higher energies.

4. Pre-equilibrium model predictions

The basic concepts of pre-equilibrium theory rest on the intranuclear cascade (INC) model of Goldberger [29] and Metropolies *et al* [30] and the statistical model of intermediate structure (SMIS) of Griffin [1]. Much effort has been devoted to combining both into a single one capable of calculating absolute pre-equilibrium emission cross-sections. In hybrid model [4] the pre-equilibrium emission spectra are given by simple closed formed expressions. However, the index model [10] involves more complex recursion relations. The index model, which is an acronym for *ind*ependently interacting *ex*citon model, has a somewhat different philosophy than the hybrid model. Both the models constitute significantly different approaches and yield different results for the pre-equilibrium emission but still they are built on the same basic assumption concerning the physics of the reaction.

The principal idea incorporated in the index model is nearly the same as in the hybrid model. The deexcitation cascade followed by individual excitons is independent of each other. However, the corresponding use of single particle state lifetimes implies a different statistical treatment for the higher stages of the nuclear equilibration than in the hybrid model. As far as particle emission is neglected, the internal collisions of all excitons of the initial configuration $n_0(p_0, h_0)$ lead to $n_1 = 3n_0$ excitons in the next stage, since each decaying exciton at a particular excitation energy loses part of its energy to create an additional particle-hole pair. The particle and hole number becomes $p_1 = 2p_0 + h_0$ and $h_1 = p_0 + 2h_0$. Due to this multiplicative proliferation factor three, instead of the additive constant two in the hybrid model, the number of excitons quickly increases from stage to stage so that two or three stages suffice to yield the total pre-equilibrium cross-section. The particle and hole densities of subsequent stages are derived from preceding stages using recursion relations.

The observed excitation functions show a high energy tail following the usual compound nucleus bump at low energy. The calculation starts with an initial number of excitons, i.e. particles above and holes below the fermi level, induced by the primary interaction and proceeds to states with an increasing exciton number. For each of these states the emission probability for the particles is calculated and finally the integrated spectra yield the cross- sections for the individual reactions. The statistical part of the codes (Overlaid Alice) can account for a large variety of reaction types. Besides evaporation of neutrons and protons [19] also clusters such as deuteron and alpha particles can be considered.

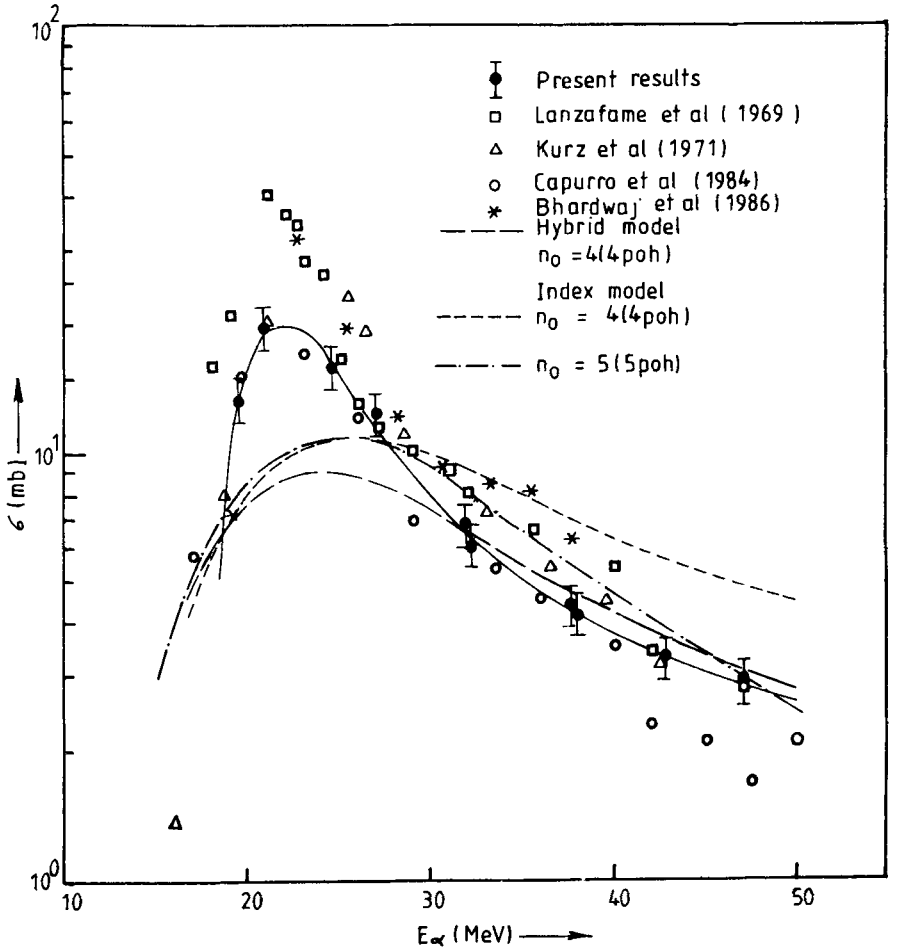

Figure 1. Excitation function of $^{197}Au(\alpha, n)^{200}Tl$ reaction.

A short description of the option chosen is given below. The nuclear masses were calculated from the Myers–Swiatecki mass formula [31] considering liquid drop with shell correction term without pairing, i.e. the level density pairing shift absorbed in binding energies. The inverse cross-sections were calculated by an optical model subroutine included in the code, where the optical model parameters were those of Becchetti and Greenless [32]. The fermi level density used is of the form

$$\rho(u) \propto (u-\delta)^{-5/4} \exp[2\sqrt{a(u-\delta)}]$$

where u is residual nucleus excitation, a is the level density parameter taken as A/8 MeV^{-1} which is the default option of the code and $\delta = 11/\sqrt{A}$ MeV the pairing energy shift.

In the *a priori* formulation of the hybrid and index models, the intra-nuclear transition rates are calculated either from the imaginary part of the optical model or from the free nucleon-nucleon scattering cross-section [33]. The use of optical potential in calculating intra-nuclear transition rates for pre-equilibrium decay models offers distinct advantages at least in principle over the nucleon-nucleon scattering approach.

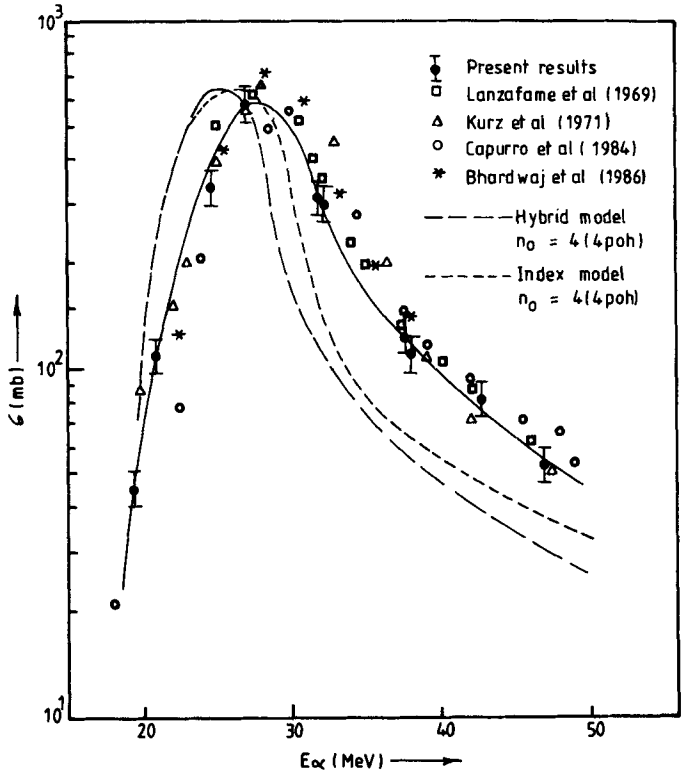

Figure 2. Excitation function of $^{197}Au(\alpha, 2n)^{199}Tl$ reaction.

Specifically, the parameters of the optical potential have been determined from the results and trends of a large body of experimental data. The mean free path values are therefore based on experimental measurements in nuclear matter as opposed to the extrapolation of free scattering cross-sections to the nuclear environment. Secondly the question of possible errors in nucleon-nucleon scattering approach due to inability to consider recoil momentum effects are avoided by using the optical potential. Becchetti and Greenless [32] have analysed large amount of data to find a best set of optical model parameters for nucleon induced reactions. But for particle energies exceeding 55 MeV the optical model parameters of Becchetti and Greenless are no longer applicable and thus at higher energies the calculation of the mean free path for intra-nuclear transitions is done from nucleon-nucleon scattering cross-sections.

The mean free path multiplier K which is a kind of free parameter introduced by Blann [34] to account for the transparency of nuclear matter in the lower density nucleus periphery was kept as unity.

The initial exciton number $n_0(p_0h_0)$ plays an important role because it governs the entire cascading process of the binary collisions and thereby influences the shape of the hard component in the particle spectra. A good guess would be the number of nucleons in the projectile or an additional particle/hole or both [10, 27, 28, 35]. This view is quite consistent with the basic physics of the pre-equilibrium decay that only a small number of degrees of freedom is initially excited in nuclear reactions at moderate energies. So, we have made the theoretical calculations using $n_0 = 4(4p0h)$, $n_0 = 5(5p0h)$ and

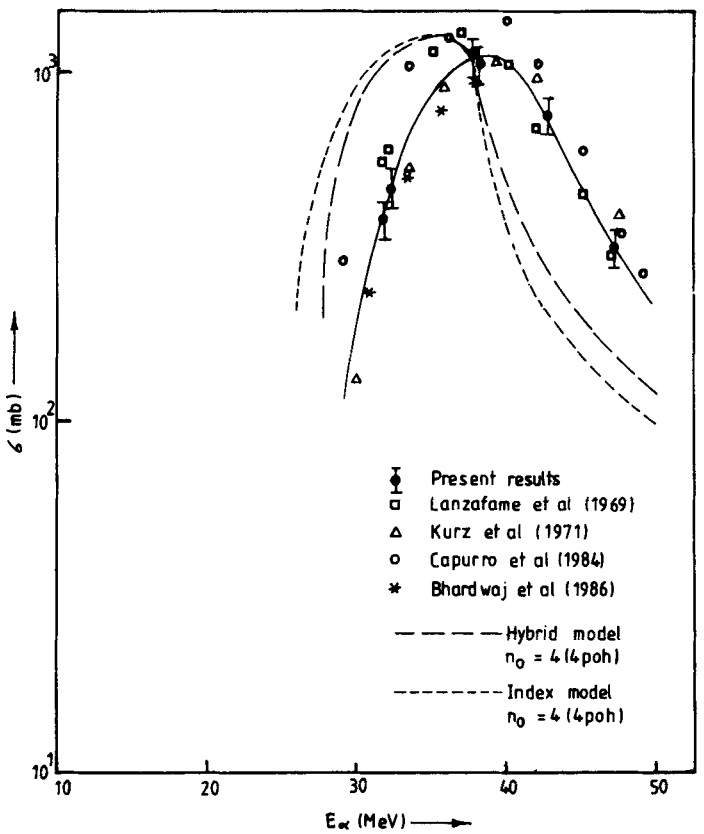

Figure 3. Excitation function of ^{197}Au$(\alpha, 3n)^{198}$Tl reaction.

$n_0 = 6(5p1h)$ as initial configurations. In view of this, a set of six theoretical excitation functions is calculated for each reaction using the three values of n_0, in the framework of two models. All these are tested against the experimentally measured excitation function to pick out the best out of them and to draw inferences based on these comparisons individually for each reaction at first. In general, it was found that $n_0 = 4(4p0h)$ gives by far the best results for both models. The prediction of the $n_0 = 5(5p0h)$ and $n_0 = 6(5p1h)$ configurations were lower than those obtained with $n_0 = 4(4p0h)$.

Figures 1–3 and 5 show a comparison of the present experimental results with hybrid and index models predictions. The lines (i.e. solid, broken and dashed lines) are drawn only to guide the eye. It can be seen from figure 1 that Au(α, n) reaction is fairly well reproduced by hybrid model, whereas index model makes an overestimation by a factor of two using $n_0 = 4(4p0h)$ in the high energy region (30–50 MeV) where the pre-equilibrium effect is predominant. It is observed that the index model gives fairly good account of high energy region with initial exciton configuration $n_0 = 5(5p0h)$, but both the models failed to account the compound nucleus part. The excitation functions of reactions Au$(\alpha, 2n)$ and Au$(\alpha, 3n)$ are shown in figures 2 and 3. It can be seen that the theoretical shape of excitation function using initial exciton configuration $n_0 = 4(4p0h)$ agrees well with the experimental shape of excitation function, there is a systematic underestimation by about 30 to 40% of the experimental cross-sections at high energy region.

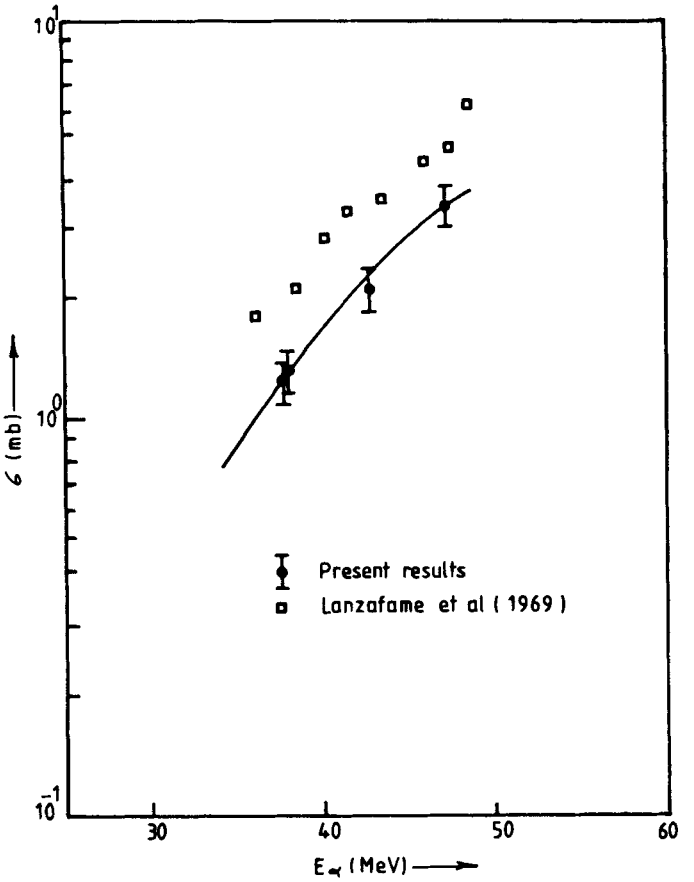

Figure 4. Excitation function of $^{197}Au(\alpha, 2pn)^{198}Au$ reaction.

It is well-known that value of a shows local variations, particularly in the vicinity of magic numbers, thereby affecting the compound nucleus part of the cross-section dominating at lower energies. Consequently, the maximum in the experimental excitation function occurring due to the compound nucleus is matched with theoretical Weisskopf–Ewing estimate by adjusting the value of the level density parameter approximately. We varied level density a as A/7, A/8, A/9, A/10, A/11 and A/12 MeV^{-1} to reproduce the compound nucleus peaks respectively after fixing the initial exciton configuration n_0. However, all the six values of level density parameter are not able to match the experimental compound nucleus peak of excitation function (figure 1). The variation is only about 10%. Based on these considerations, the value of the level density parameter a for theoretical calculations was chosen as the global parameter A/8 MeV^{-1}.

As far as $^{197}Au(\alpha, 2pn)$ reaction is concerned, (figure 4) the observed experimental cross-sections between 30 and 50 MeV cannot be accounted for either by equilibrium or pre-equilibrium mechanisms using hybrid and index models.

Figure 5 shows the excitation function of the $^{179}Au(\alpha, \alpha n)$ reaction. There is a radical difference in the shape of theoretical and experimental excitation functions, as well as severe underestimation of the theory by two orders of magnitude. This is of course not very surprising because, neither the hybrid model nor the index model, is designed to

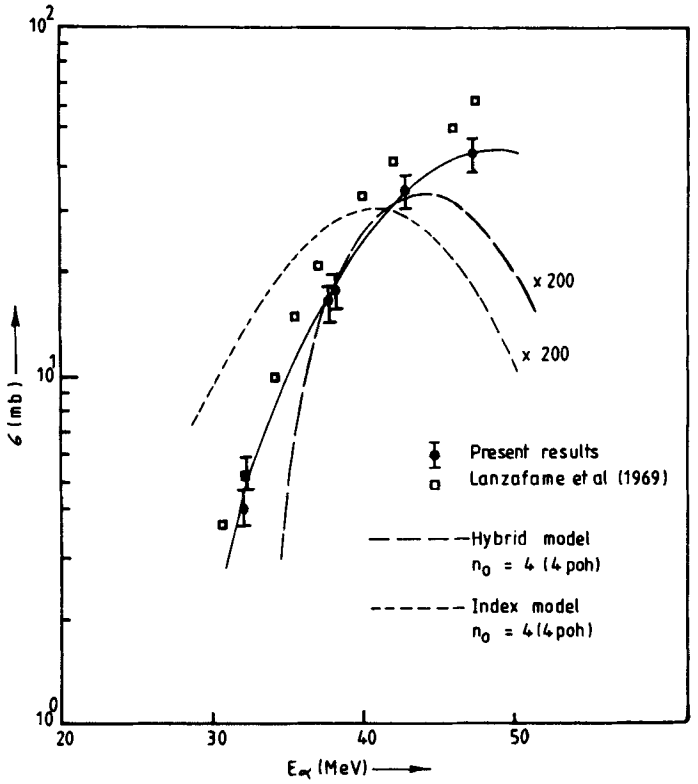

Figure 5. Excitation function of $^{197}Au(\alpha, \alpha n)^{196}Au$ reaction.

deal with alpha particle emission in the pre-equilibrium phase, which is quite likely at moderate energies.

Further, as seen in the figures there is a slight shift in the energy between the theoretical and experimental compound nucleus peak. Generally such shifts are ascribed due to the complete neglect of angular momentum effects in the Weisskopf–Ewing theoretical calculations provided in the codes. More elaborate computations, using Hauser–Feshbach theory [36] may bring about a better agreement.

5. Conclusion

From the present study of the excitation functions for $^{197}Au(\alpha, xnypz\alpha)$ reactions, it is concluded that there is a qualitative agreement between our experimental results and the theoretical ones. In the observed high-energy tail of the excitation functions of the (α, xn) reactions, there are the veritable signatures of pre-equilibrium decay, irrespective of any model or theory. The basic tenet that only a small number of degrees of freedom is excited in pre-equilibrium reactions is amply borne out by the satisfactory agreement observed between the experimental results and the pre-equilibrium hybrid and index models predictions for an initial exciton number $n_0 = 4(4p0h)$ except for (α, n) reaction whereas index model with exciton number $n_0 = 5(5p0h)$ gives fairly good agreement. Comparatively speaking, the former model is better than the latter.

It can be seen from figures that there is a clear shift in energy between theoretical and experimental compound nucleus peaks. Generally such shifts are ascribed to the complete neglect of angular momentum effects in the Weisskopf–Ewing theoretical calculations of the compound nucleus contribution.

Acknowledgements

The authors are thankful to the entire staff of IUC-DAEF, Calcutta Centre and VECC Calcutta for their co-operation in the present investigation. They also wish to thank Prof. J Rama Rao and Prof. D R S Somayajulu for stimulating discussions. This work is supported by University Grants Commission, New Delhi.

References

[1] J J Griffin, *Phys. Rev. Lett.* **17**, 478 (1966)
[2] G D Harp, J M Miller and B J Berne, *Phys. Rev.* **165**, 1166 (1968)
[3] M Blann, *Ann. Rev. Nucl. Sci.* **25**, 123 (1975)
[4] M Blann and H K Vonach, *Phys. Rev.* **C28**, 1475 (1983)
M Blann code ALICE/85/300, UCID-20169 (1984)
[5] E Gadioli, E Gadioli-Erba and P G Sona, *Nucl. Phys.* **A217**, 589 (1973)
[6] J Ernst and J Rama Rao, *Z. Phys.* **A281**, 129 (1977)
[7] G Mantzouranis, D Agassi and H A Weidenmueller, *Z. Phys.* **A27**, 145 (1976)
[8] H Machner, *Phys. Lett.* **B86**, 129 (1979)
[9] J M Akkermans, H Gruppelaar and G Reffo, *Phys. Rev.* **C22**, 73 (1980)
[10] J Ernst, W Friedland and H Stockhorst, *Z. Phys.* **A328**, 333 (1987); **A333**, 45 (1989)
[11] H Feshbach, A Kerman and S Koonin, *Ann. Phys.* **125**, 429 (1980)
[12] D Agassi, H A Weidenmueller and G Mantzouranis, *Phys. Rev.* **22**, 145 (1975)
[13] T Tamura, T Udagawa, D H Feng and K K Kan, *Phys. Lett.* **B68**, 109 (1977)
[14] L Avaldi, R Bonetti and L Colli Milazzo, *Phys. Lett.* **B94**, 463 (1980)
[15] G M Field, R Bonetti and P E Hodgson, *J. Phys.* **G12**, 93 (1986)
[16] C K Cline, *Nucl. Phys.* **A210**, 590 (1973)
[17] E Betak and J Dobes, *Z. Phys.* **A279**, 319 (1976)
[18] J Bisplinghoff, *Phys. Rev.* **C33**, 1569 (1986)
[19] V F Weisskopf and D H Ewing, *Phys. Rev.* **57**, 472 (1940)
[20] F M Lanzafame and M Blann, *Nucl. Phys.* **A142**, 545 (1970)
[21] H E Kurz, E W Jasper, K Fischer and F Hermes, *Nucl. Phys.* **A168**, 129 (1971)
[22] O A Capurro, M de la Vega Vedoya, C Wasilevsky and S J Nassiff, *J. Radioanal. Nucl. Chem.* **89/2**, 519 (1985)
[23] H D Bhardwaj and R Prasad, *Nucl. Instrum. Methods* **A242**, 286 (1986)
[24] H P Graf and H Muenzel, *J. Inorg. Nucl. Chem.* **36**, 3647 (1974)
[25] C E Williamson, J P Boujot and J Picard, *CENS Report*, CEA-R 3042 (1966)
[26] C M Lederer and V S Shirley, *Table of isotopes*, 7th edn. (John Wiley, New York, 1978)
[27] N L Singh, S Agarwal and J Rama Rao, *Can. J. Phys.* **71**, 115 (1993)
[28] N L Singh, B J Patel, D R S Somayajulu and S N Chintalapudi, *Pramana – J. Phys.* **42**, 349 (1994)
[29] M L Goldberger, *Phys. Rev.* **74**, 1269 (1948)
[30] N Metropolis, R Bivins, M Storm, A Turkevich, J M Miller and G Friedlander, *Phys. Rev.* **110**, 185, 204 (1958)
[31] W D Myers and W J Swiatecki, *Nucl Phys.* **81**, 1 (1966)
[32] F D Becchetti and F W Greenless, *Phys. Rev.* **182**, 1190 (1969)
[33] M Blann, *Nucl. Phys.* **A213**, 570 (1973)
[34] M Blann, *Phys. Lett.* **27**, 337 (1971)
[35] M Blann and T T Komoto, *Phys. Rev.* **C29**, 1678 (1984)
[36] W Hauser and H Feshbach, *Phys. Rev.* **87**, 366 (1952)